ELSEVIER

Ultrasound in Med. & Biol., Vol. 34, No. 1, pp. 160–165, 2008

0301-5629/08/$–see front matter

doi:10.1016/j.ultrasmedbio.2007.06.025

● *Technical Note*

DETECTION AND QUANTIFICATION OF CALCIFICATIONS IN INTRAVASCULAR ULTRASOUND IMAGES BY AUTOMATIC THRESHOLDING

E. SANTOS FILHO,* Y. SAIJO,* A. TANAKA,† and M. YOSHIZAWA‡

*Department of Medical Engineering and Cardiology, Institute of Development, Aging, and Cancer, Tohoku University, Sendai; †Faculty of Symbiotic Systems Science, Fukushima University, Fukushima; and ‡Information Synergy Center, Tohoku University, Sendai, Japan

(*Received* 18 *January* 2007, *revised* 18 *May* 2007, *in final form* 26 *June* 2007)

Abstract—An innovative application of automatic thresholding is used for the detection of calcification regions in intravascular ultrasound images. *A priori* knowledge of the acoustic shadow that usually accompanies calcification regions is used to discriminate these from other bright regions in the image. A method for the calculation of the angle of calcification has also been developed. The proposed algorithms are applied to *in-vivo* images obtained from left anterior descending coronary arteries during percutaneous transluminal coronary angioplasty (n = 14). The resulting specificity is 72% and the sensitivity 84%. The receiver operating characteristic curve, the area under the curve being equal to 0.91, is plotted to evaluate the algorithm performance. (E-mail: esmeraldo@ieee.org)

Key Words: **Image segmentation, Calcification detection, Automatic thresholding.**

INTRODUCTION

It is estimated that cardiovascular diseases cause one-third of all deaths globally. Coronary artery disease is a chronic disease in which the coronary arteries gradually harden and narrow in a process called atherosclerosis. As the heart muscle is fed with oxygen-rich blood delivered by the coronary arteries, a blockage in these arteries can cause a heart attack (WHO 2005).

Currently, several imaging modalities are available to support the diagnosis of coronary artery diseases. X-ray coronary angiography and intravascular ultrasound (IVUS) are examples of the most commonly used diagnostic tools. Intravascular ultrasound has several important advantages over angiography and provides new diagnostic and therapeutic insights into coronary disease. The tomographic orientation of ultrasound enables visualization of the entire circumference of the vessel wall and provides information about the tissues beneath the luminal border (Kaneda et al. 2003).

As presented in the work of Rao et al. (2005), the knowledge about the origin and progression of atherosclerosis has advanced greatly in the last years. However, the factors that determine atheromatous plaque instability are not well understood. New diagnostic and therapeutic methods would have to be developed if an accurate and reliable prediction of plaque vulnerability were available. Based on histologic analysis of aortas with areas of gross atherosclerosis, Rao et al. (2005) observed that plaque instability is highly correlated with intraplaque hemorrhage, lipid content and plaque size. Calcification does not seem to be a significant indicator of plaque instability.

However, the amount of coronary calcium has been shown to be very important for physicians. Shaw et al. (2006) have conducted a study that confirms the prior findings that the prevalence of coronary calcification increases with age. They evaluated a unique method whereby estimates of the extent of coronary calcification may be used to adjust a patient's age. It was revealed by their study that for elderly patients with low-risk calcium scores, survival is equivalent to that for patients 1 to 10 years younger. On the other hand, for younger patients with moderate- to high-risk calcium scores, survival is equivalent to that for patients approximately 20 years older. Thus, a score that includes coronary calcium and age may be useful for prevention strategies.

Address correspondence to: E. Santos Filho, Department of Medical Engineering and Cardiology, Institute of Development, Aging, and Cancer, Tohoku University, 4–1 Seiryomachi, Aoba-ku, Sendai 980–8575, Japan. E-mail: esmeraldo@ieee.org

The presence or absence of calcium demonstrated by IVUS has been shown to be an important determinant of transcatheter interventional success (Scott et al. 2000). In theory, there may be a critical quantity of calcium that is predictive of an unsatisfactory outcome with balloon angioplasty, but without an accurate method to quantify coronary calcification, that critical calcium content cannot be determined.

Several studies on IVUS image segmentation have been published that aim to automate this process (Saijo et al. 2004, 2006a; Sonka et al. 1995; Brusseau et al. 2004; Vince et al. 2000).

In this paper, we present an algorithm based on automatic thresholding for the automatic detection of the calcification regions in IVUS images, which may be used for the automation of the method proposed by Scott et al. (2000).

MATERIALS AND METHODS

Intravascular ultrasound data were acquired with an IVUS console (Clear View Ultra, Boston Scientific Inc., Natick, MA, USA) and a 40-MHz mechanically rotating IVUS catheter (Atlantis SR Plus, Boston Scientific Inc.). Radiofrequency (RF) data were digitized and stored on a personal computer (Dell Precision Workstation 330, Dell Inc., Round Rock, TX, USA) using an A/D board (GAGE Compuscope 8500, 500 Msamples/s, 8-bit resolution, Gage Applied Inc., Montreal, Quebec, Canada) for off-line analysis. The images used were of the Windows bitmap type and the algorithms were developed using MATLAB (The Mathworks, Inc., Natick, MA, USA).

Subsequently, the RF signal was preprocessed and converted to a conventional B-mode IVUS image through a software developed by our group. Using this procedure we could remove the influence of the control settings of the IVUS console that usually affect algorithms based on image gray levels.

Radiofrequency signal data were acquired *in vivo* from 14 human left anterior descending (LAD) coronary arteries during percutaneous transluminal coronary angioplasty (PTCA). This process was approved by a local investigation review board and was performed in accordance with the ethical principles for medical research involving human subjects. We obtained written informed consent from all subjects.

Multithresholding segmentation

Calcification regions are usually very bright regions in IVUS images. Tests using speed of sound microscopy (Saijo et al. 2006b) have confirmed that the strongest echo is produced between calcium and lumen or calcium and media, where the difference in the specific acoustic impedance is large.

Thus, it is natural to consider thresholding as a simple method to segment calcification regions. However, in spite of being brighter compared with normal tissue, the gray levels of the calcified regions and normal tissue usually change from image to image. This fact makes it very difficult to determine a single threshold value capable of accurately segmenting a series of images.

Thus, it is necessary to adapt the threshold level for each input image. In this work, we used the Otsu method (Otsu 1979) to automatically find the optimal threshold for each image. However, in our tests, applying thresholding only once was not sufficient to obtain segmented regions that were reasonably close to the regions of calcification.

To solve this problem, a multithresholding method was applied, using successive applications of the Otsu method as summarized in the following algorithm. The Otsu method is summarized in the Appendix.

Algorithm 1. Step 1: Compute the histogram.

Step 2: Compute the optimal threshold $k*$ that maximizes the between-class variance $\sigma_B^2(k)$.
$\sigma_B^2(k^*) = \max\sigma_B^2(k)$

Step 3: Compute a new histogram for $i \geq k*$.

Step 4: Go to step 2.

After several tests, it was observed that three iterations of the above algorithm were sufficient to obtain segmentation sufficiently close to the regions of calcification.

However, often normal tissue, parts of the catheter and artifacts also form very bright regions and may be wrongly segmented. For this reason, it is necessary to develop a method to ignore segmented bright regions that are not calcifications.

Identification of calcification from the regions-of-interest

Another characteristic of calcification regions is that they are usually accompanied by an acoustic shadow as a result of the high reflection of the ultrasound beam at such sites. Thus, an effective way to detect whether a given segmented bright region, hereafter called a region-of-interest (ROI), is a calcification region, is through the analysis of the region behind the ROI. In Fig. 1, there is an example of an IVUS image with a calcification region and a graph of the median gray level of the pixels in each column of the corresponding polar coordinate system image.

We can observe in Fig. 1 that the region of calcification is accompanied by an acoustic shadow, and the corresponding region in the graph presents a lower median level.

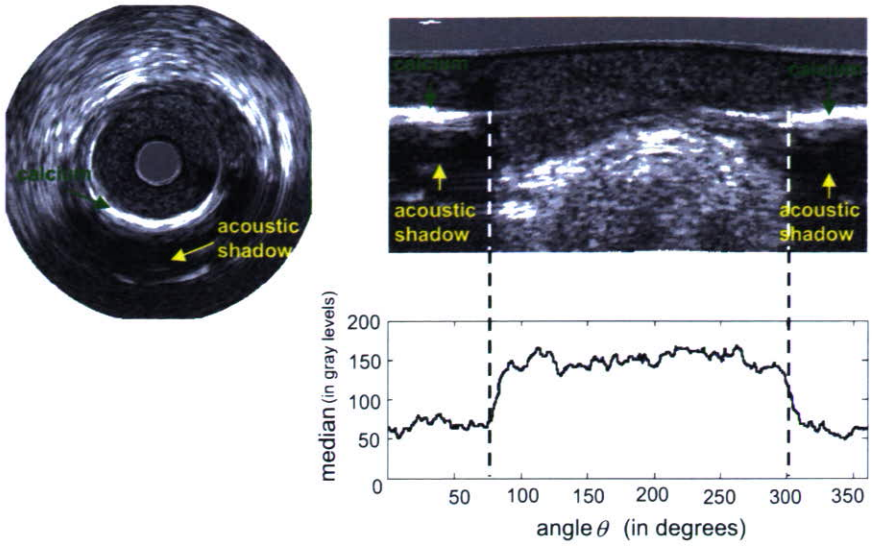

Fig. 1. Example of an IVUS image with a calcification and its corresponding graph of median gray level of the pixels in each column of the rectangular coordinates system corresponding to the original polar system of IVUS images.

Detection of acoustic shadow

To detect the acoustic shadow and then determine whether a given ROI is a calcification, the following algorithm is used:

Algorithm 2. Step 1: Determine the centroid of the segmented ROI.

Step 2: From the centroid of the ROI to the bottom of the image (pixels of the yellow line in Fig. 2), calculate the median gray-level value, *Med*.

Step 3: If $\frac{Med}{M_{cent}} \leq T_{med.}$ then classify the ROI as a calcification. Otherwise, classify the ROI as a noncalcification region. M_{cent} denotes the gray level of the pixel at the centroid of the ROI.

T_{med} was chosen based on tests using several images. As illustrated in Fig. 2, only ROI 2 was selected as a calcification region because of its detected acoustic shadow.

The true-positive rate and the false-positive rate depend on the threshold value T_{med} used to define positive and negative test results. As we shift T_{med} in the range of the possible values of $\frac{Med}{M_{cent}}$ found in our tests (from 0.3 to 0.98), the true-positive rate and false-positive rate also present increasing values, which are used to construct the ROC curve. Some values are shown in Fig. 5 as examples.

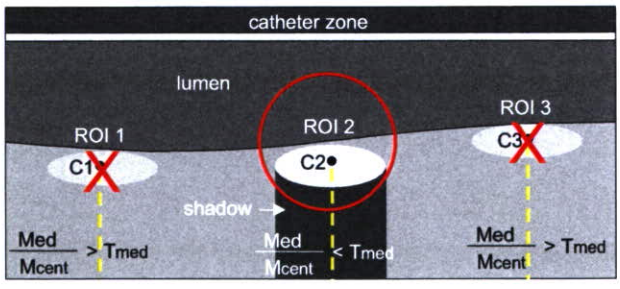

Fig. 2. Example of identification of calcification due to acoustic shadow. The ROI 1 and ROI 2 were not classified as calcification (indicated by the red X). The ROI 2 was classified as calcification (indicated by the red circle). The criterion for classification was the presence of acoustic shadow detected through analysis of the pixels in the yellow line. ROI = region of interest; C = centroid.

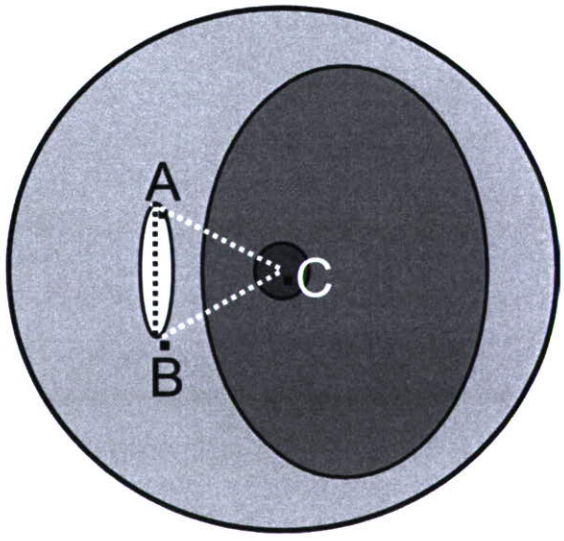

Fig. 3. Example of determination of the angle of calcification. (A) and (B) are the extreme points of the calcification region. (C) is the center of the catheter.

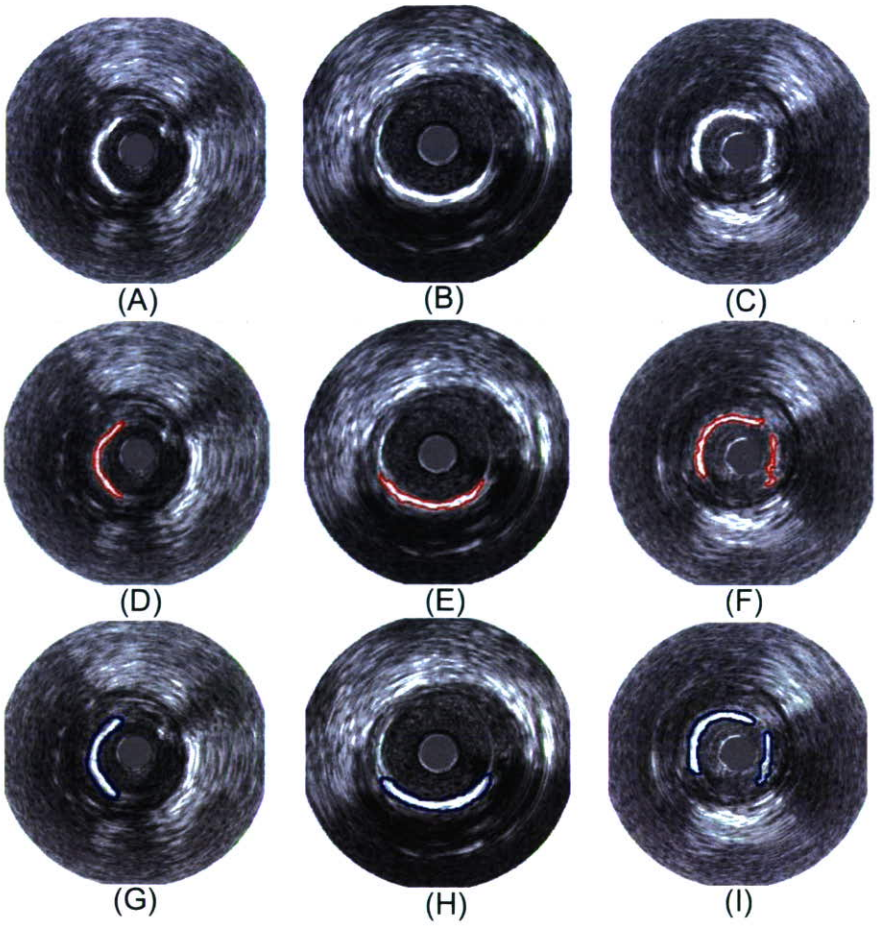

Fig. 4. Example of calcification regions automatically segmented. (A, B, C) Original images. (D, E, F) Corresponding automatically segmented images. (G, H, I) Corresponding manually segmented images. The outlined areas are the calcification regions.

Quantification of calcification regions

Usually, the method used to quantify calcium through IVUS images is based on the arc of calcium measured in a single frame of the IVUS movie of the site of the calcification. However, the accuracy of this method would be increased if it could take into account the extent of the total epicardial coronary calcium (Scott et al. 2000).

Scott et al. (2000) have proposed a method for calcification quantification similar to Simpson's rule, which is used in calculus to determine volumes. As a sequence of known areas separated by a known distance can be used to calculate volume, a sequence of known circumferences separated by a known distance can be used to calculate the surface area.

As the manual measurement of calcification across a sequence of frames is a tedious and time-consuming task, we developed an algorithm for the measurement of the angle of the calcification regions detected through the automatic thresholding. This method is summarized in the following algorithm:

Algorithm 3. Step 1: Determine the extreme points of the calcification region denoted by the letters A and B, as shown in Fig. 3.

Step 2: Determine the center of the image (center of the catheter), denoted by the letter C, and then calculate the length of the sides of the triangle determined by points A, B and C.

Step 3: Using the sine and cosine rules, calculate the angle whose vertex is at point C; this will be considered as the calcification angle.

Intravascular ultrasound sequences containing calcification regions were selected by an expert medical doctor, and from each calcification region sequence, one representative frame was selected for the tests. Then, the selected images were manually segmented by the expert medical doctor and used as our gold standard.

RESULTS

Using the algorithms for automatic thresholding and acoustic shadow detection, tests were performed and

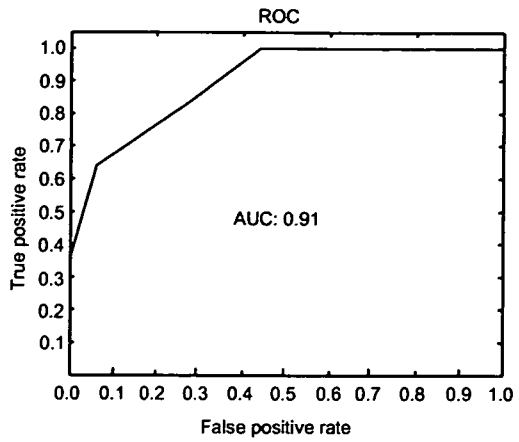

Example of ROC curve points

threshold	TPR	FPR
0.3	0.36 (9/25)	0.0 (0/18)
0.4	0.64 (16/25)	0.06 (1/18)
0.5	1.0 (25/25)	0.44 (8/18)

Fig. 5. Receiver operating characteristic curve. The AUC is equal to 0.91. TPR = true-positive rate; FPR = false-positive rate.

some of the results are shown in Fig. 4. We observe that in these images, the regions of calcification are segmented accurately. The threshold level used for the median values is empirically determined as $T_{med} = 0.45$. Table 1 summarizes the results of the tests, and the ROC curve is plotted in Fig. 5. The area under the curve (AUC) is equal to 0.91. The resulting specificity is 72% and the sensitivity 84%.

DISCUSSION

The analysis of the images in the rectangular coordinate system (demodulate RF line) corresponding to the originally polar system of the IVUS images facilitates the process of acoustic shadow detection because in the rectangular images, the shadow region is confined to a given number of columns, forming a rectangular area that can be scanned easily.

Sometimes part of the catheter may appear very bright and simultaneously present an acoustic shadow because of the presence of the guide wire. In such cases, part of the catheter may be wrongly segmented as a calcification. To prevent this problem, a test is performed to determine whether the centroid of the ROI is inside the 30-pixel-length radius circle centered at the catheter center. This circle corresponds, approximately, to the catheter region. Thus, if a ROI centroid falls inside this circle, it will not be considered as a candidate calcification region. However, because of this constraint, an underestimation of the amount of calcium may occur in the case of a highly concave calcification region that is very close to the catheter, causing its centroid to fall inside the catheter region. In this case, this calcification will not be detected. However, in our tests we did not find such a case.

Table 1. Table of results

	ROIs correctly classified	ROIs wrongly classified	Total number of ROIs
Calcification	21	4	25
Normal tissue	13	5	18

ROI = Region-of-interest.

The number of iterations of successive thresholding was determined empirically. It was observed that after each threshold, the value of the standard deviation of the gray level in the remaining regions usually declines. This information may be used to define a stopping criterion and then improve the robustness of the proposed algorithm.

In frames without calcification regions, the ROIs remaining after the third thresholding are usually very few in number and very small in size. Furthermore, in these images, the gray level declines smoothly away from the ROI. Thus, the gray level at the centroid of these ROIs and the gray levels in their neighborhood are usually very close; this makes the value $\frac{Med}{M_{cent}}$ approach unity and cause the ROIs to be classified as noncalcification regions.

The results were evaluated through visual inspection by the expert who also traced the manually segmented contours. In spite of some differences between the areas of the ROIs manually and automatically traced, the results were considered accurate because the parameter to be quantified was the length of the arc of the segmented calcification. The thickness of the segmented region was ignored because the ultrasound beam is almost completely reflected at the surface of the calcification regions and causes a shadow that makes it difficult to assess the real thickness of the calcification.

The false positives were caused by the presence of the guide-wire shadow. However, it is possible that regions of fibrosis may also be sufficiently bright compared with other tissues to cause $\frac{Med}{M_{cent}} \leq 0.45$ and be wrongly considered as calcifications. However, in our tests we did not find such a case.

The center of the vessel is the point that should be used for the calculation of the angle of the calcification. However, to find this center, it would be necessary to first accurately find the luminal contour. In our tests, the center of the image was used as an approximation of the center of the vessel.

As future work, the proposed algorithm may be combined with other existing methods for luminal contour segmentation, becoming an important step toward the full automation of the method proposed by Scott et al. (2000).

Acknowledgements—This study was supported by the Grants-in-aid from the Ministry of Health, Labour and Welfare of Japan (H17-nano-001).

REFERENCES

Brusseau E, Korte CL, Mastik F, Schaar J, van der Steen AFW. Fully automatic luminal contour segmentation in intracoronary ultrasound imaging—A statistical approach. IEEE Trans Med Imaging 2004;23:554–566.

Kaneda H, Honda Y, Yock PG, Fitzgerald PJ. What do cardiologists want from vascular ultrasound. In: Saijo Y, van der Steen AFW,eds. Vascular Ultrasound. Tokyo: Springer-Verlag, 2003:3–27.

Otsu N. A threshold selection method from gray-level histograms. IEEE Trans Systems Man Cybernectics 1979;9:62–66.

Rao DS, Goldin JG, Fishbien MC. Determinants of plaque instability in atherosclerotic vascular disease. Cardiovasc Pathol 2005;14:285–293.

Saijo Y, Tanaka A, Owada N, Akino Y, Nitta S. Tissue velocity imaging of coronary artery by rotating-type intravascular ultrasound. Ultrasonics 2004;42:753–757.

Saijo Y, Tanaka A, Iwamoto T, et al. Intravascular two-dimensional tissue strain imaging. Ultrasonics 2006a;44:e147–151.

Saijo Y, Hozumi N, Lee C, et al. Ultrasonic speed microscopy for imaging of coronary artery. Ultrasonics 2006b;44:e51–55.

Scott DS, Arora UK, Farb A, Virmani R, Weissman NJ. Pathologic validation of a new method to quantify coronary calcific deposits in vivo using intravascular ultrasound. Am J Cardiol 2000;85:37–40.

Shaw LJ, Raggi P, Berman DS, Callister TQ. Coronary artery calcium as a measure of biologic age. Atherosclerosis 2006;188:112–119.

Sonka M, Zhang X, Siebes M, et al. Segmentation of intravascular ultrasound images: A knowledge-based approach. IEEE Trans Med Imaging 1995;14:719–732.

Vince D, Dixon K, Cothren R, Cornhill J. Comparison of texture analysis methods for characterizations of coronary plaques in intravascular ultrasound images. Comput Med Imaging Graph 2000; 24:221–229.

World Health Organization. Cardiovascular diseases. Available at: http://www.who.int/topics/cardiovascular_diseases/en/. Accessed June 11, 2005.

APPENDIX

Automatic threshold estimator

Otsu (1979) developed an optimal threshold selection method based on the maximization of the separability of the resultant classes. His procedure is very effective and utilizes only the 0^{th} and first-order cumulative moments of the gray-level histogram. Thus, because of its simplicity and effectiveness, the Otsu method was used as the threshold estimator in this work.

Following Otsu's formulation, let the pixels of a given image be represented in L gray levels $[1, 2, \cdots, L]$. The number of pixels at gray level i is denoted by n_i and the total number of pixels by $N = n_1 + n_2 + \cdots + n_L$. After normalization, the gray-level histogram may be regarded as a probability distribution:

$$p_i = n_i/N \tag{1}$$

$$p_i \geq 0, \sum_{i=1}^{L} p_i = 1 \tag{2}$$

We separate the pixels into two classes, C_0 and C_1 (background and object or *vice versa*), by a threshold at gray level k; C_0 denotes pixels with gray levels $[1, \cdots, k]$ and C_1 denotes pixels with levels $[k + 1, \cdots, L]$. Then, the probabilities of class occurrence and the class mean gray levels, respectively, are given by:

$$\omega_0 = \Pr(C_0) = \sum_{i=1}^{k} p_i = \omega(k) \tag{3}$$

$$\omega_1 = \Pr(C_1) = \sum_{i=k+1}^{L} p_i = 1 - \omega(k) \tag{4}$$

and

$$\mu_0 = \sum_{i=1}^{k} i\Pr(i|C_0) = \sum_{i=1}^{k} ip_i/\omega_0 = \mu(k)/\omega(k) \tag{5}$$

$$\mu_1 = \sum_{i=k+1}^{L} i\Pr(i|C_1) = \sum_{i=k+1}^{L} ip_i/\omega_1 = \frac{\mu_T - \mu(k)}{1 - \omega(k)}, \tag{6}$$

where

$$\omega(k) = \sum_{i=1}^{k} p_i \tag{7}$$

and

$$\mu(k) = \sum_{i=1}^{k} p_i \tag{8}$$

are the 0^{th} and first-order cumulative moments of the histogram up to the k^{th} level, respectively, and

$$\mu_T = \mu(L) = \sum_{i=1}^{L} ip_i \tag{9}$$

The optimal threshold is defined (Otsu 1979) as the value that maximizes the between-class variance

$$\sigma_B^2(k) = \frac{[\mu_T\omega(k) - \mu(k)]^2}{\omega(k)[1 - \omega(k)]} \tag{10}$$

Thus, the optimal threshold $k*$ is given by:

$$\sigma_B^2(k^*) = \max_{1 \leq k < L} \sigma_B^2(k) \tag{11}$$